

Fabrication of Hybrid Solar Cells using Poly (2,5-dimethoxyaniline) Hexagonal Structures and Zinc Oxide Nanorods

S. E. Mavundla^{a,*}, G. F. Malgas^b, D. E. Motaung^b, E. I. Iwuoha^c

^aSchool of Engineering, Department of Chemical Engineering, University of South Africa, Florida campus, Private Bag X6, Florida 1710, South Africa

^bDST/CSIR, Nanotechnology Innovation Centre, National Centre for Nano-Structured Materials, Council for Scientific and Industrial Research, P. O. Box 395, Pretoria, 0001, South Africa

^cSensor Lab, Department of Chemistry, University of the Western Cape, Private Bag X17, Bellville 7535, South Africa

ABSTRACT

Flower-shaped zinc-oxide (ZnO) structures have been synthesized in a microwave at 180 °C for 20 min using zinc nitrate and KOH. Detailed structural and morphology observations showed that the micron-size ZnO nano-pencils grow out of the base of the flower-shaped ZnO structures. Photoluminescence spectra measured at room temperature showed a sharp UV emission band around 390 nm, attributed to the radiative annihilation of excitons. The synthesized PDMA and ZnO nanopencils are highly crystalline materials with a one-dimensional morphology which improves the electron charge transport in the device. A distinctive photoluminescence quenching effect is observed indicating a photo-induced electron transfer. The solar cell devices fabricated from these materials demonstrated a short circuit current density of 0.93 $\mu\text{A}/\text{cm}^2$, an open-circuit voltage of 0.58 V and an efficiency of 0.16%.

Key words: nanopencils, copolymers, nanorods, organic solar cells

1. INTRODUCTION

Since the introduction of a two layered organic solar cells by Tang [1], organic solar cells have undergone a gradual evolution that has led to energy conversion efficiencies of more than 6%

* Corresponding Author: Dr. Siphon Mavundla, Tel: (+27) 11 471 3215, Fax: (+27) 86 764 1651, Email: mavunse@unisa.ac.za

[2]. Although organic solar cells show low efficiencies, the simplicity of the devices and the potential to increase efficiencies makes them worthwhile prospects for research and development [3]. The weak absorption in the visible long wavelength, poor charge transport and low stability are some of the reasons for the poor performance of organic solar cells. The transport of the charges after their separation simply relies on the percolation network of the components of the mixture films, which is not easy to control precisely through dynamic coating or simple thermal annealing [3].

One way to improve charge transport is to replace one of the organic components by an inorganic material. These types of devices are called hybrid solar cells. The advantages of hybrid solar cells over purely organic counterparts are environmental stability, high electron transport, and the ability to optimize interfacial properties [4]. The control of morphology of inorganic semiconductors from spherical to one dimensional structure is attractive for solar cell application because of their ability to provide direct path for charge transport [5, 6]. It has been previously shown that photo-induced charge transfer can also occur between a conjugated polymer and a metal oxide semiconductor such as tin oxide (SnO_2), titanium oxide (TiO_2), and zinc oxide (ZnO) [7]. Among metal oxides, ZnO is one of the most studied material because of its easy synthesis process, tunable morphology, wide band gap, low- cost, and high mobility. On the other hand polyaniline is one of the most studied polymers due to its high conductivity, environmental stability and low cost of production [8]. Polyaniline can also act as a barrier to oxygen and as a planarizing layer to inhibit electrical shorts and improve device lifetime, resulting in an improvement of the brightness and the efficiency of the Organic Light Emitting Diodes [9]. It has been shown that by incorporating a one dimensional structure of polyaniline as an interfacial layer in organic solar cell, the efficiency can be improved by up to 26% [10]. In this work, we report on the synthesis of one-dimensional ZnO -nanopencils and its comparison with C_{60} as electron acceptor materials in fabricating hybrid solar cells of poly(2,5-dimethoxyaniline)(PDMA) and poly(2,5-dimethoxyaniline-pyrrole)(PDMA-PPy).

2. EXPERIMENTAL

2.1. Materials

Zinc nitrate, potassium hydroxide (KOH), dimethylformamide (DMF, 99%), buckminsterfullerene C_{60} with a purity of 99.5%, Indium tin oxide (ITO) coated on a 1 mm glass substrate with a sheet resistance of 8 - 12 Ω/sq^{-1} , poly(3,4-

ethylenedioxythiophene):poly(styrenesulfonate) (PEDOT:PSS) (99% purity) and hydrochloric acid (HCl) were purchased from Sigma-Aldrich. All chemicals were used as received without further purification.

2.2. Synthesis of ZnO nanostructures

ZnO nanostructures were prepared by dissolving 4.8 g of Zinc nitrate in 50 mL of deionised water. A 4 g of the KOH was added with continuous stirring to make a colloidal solution. The resulting solution was then transferred to a 100 mL Teflon liner and put in a vessel. The solution was heat treated at a temperature of 180 °C for 20 min in a microwave under temperature controlled mode. The solution was cooled down to room temperature and the final products were dried at 80 °C. DMA and PDMA-PPy were synthesized as described in references [8] and [11] respectively.

2.3. Fabrication of devices

For solar cell device fabrications, the ITO glass substrates were ultrasonically cleaned with methanol for 5 min. Photoactive layers were prepared by mixing PDMA:ZnO, PDMA-PPy:ZnO or PDMA-PPy:C₆₀ in a 1:1 weight ratio and dissolved in 2 mL of DMF. To attain a complete dissolution between the polymer and blends, the solutions were stirred overnight at 50 °C. For device fabrication a thin layer of PEDOT:PSS solution was spin coated onto the ITO glass substrates. This was followed by thermal treatment of the PEDOT:PSS/ITO substrates at 100 °C for 20 min. The active layer consisting of the polymer blends was spin-coated on top of the PEDOT:PSS/ITO glass substrates and dried at 50 °C for 30 min.

Solar cells were prepared by depositing a aluminum (Al) top electrode on top of an ITO glass substrate. This glass/ITO/Al substrate was placed on top of the ITO/PEDOT:PSS/PDMA:ZnO substrate with an appropriate displacement and laminated together by applying a certain pressure at a controlled temperature using a hydrostatic pressurizer with hot plates (AH-1TC,ASONE,Japan).

2.4. Characterization

Microwave synthesis was performed on a Perkin Elmer/Anton Paar Multiwave 3000. The scanning electron microscopy (SEM) samples were prepared by placing some of the synthesized material onto an aluminum stub. A carbon sticky tape was placed on the aluminum stub for adhesion

of the material. The samples were sputter-coated with a thin layer of carbon to prevent charging effects inside the microscope. The morphology of the prepared materials was examined on a Neon 40 (Zeiss) FIB-SEM. Ultraviolet-visible (UV-Vis) spectra were recorded on a PerkinElmer Lambda 750S spectrometer from 320 to 900 nm. Photoluminescence (PL) measurements were recorded on PerkinElmer LS 55 spectrometer by exciting the samples with a 320 nm line of deuterium lamp. The UV-Vis and PL samples were prepared by dissolving a small amount of the material in DMF. The X-ray diffraction patterns of the powders were recorded on a Phillips (PANalytical) X-ray diffractometer using a Cu K α ($\lambda = 1.54\text{\AA}$) radiation source. The measurements were extracted at 45.0 kV and 40.0 mA. Data were obtained from $2\theta = 5$ to 40° with a step size of 0.02° . The current-voltage (IV) characteristics were measured using a Keithley 4200 Semiconductor Characterization System. The devices were irradiated at 80 mW cm^{-2} using a Sciencetech SF150 solar simulator equipped with a xenon short arc lamp with a power of 150 W. . . The optical power at the sample was 80 mW cm^{-2} , detected using a daystar meter. All the photovoltaic properties were evaluated in ambient air conditions at room temperature.

3. RESULTS AND DISCUSSION

3.1. Scanning Electron Microscopy

Figure 1 shows the scanning electron microscopy (SEM) images of the as-grown products of ZnO, PDMA and PDMA-PPy. The micrographs in Figure 1a and b show the ZnO structures with a hexagonal behaviour with a tip shape morphology which might have a significant application in field emission, scanning probe microscopy (SPM) and highly sensitive devices [12]. It is observed from the base of the flowers that the ZnO structures (nanopencils) grow outward from the base of the material. It is noticeable that the end faces of these nanostructures are needle shaped.. Once the ZnO structures forms the pencils stop growing. These ZnO nanopencils are about 400 nm in diameter and 1.6 μm in length. Their formation can be ascribed to the fact that ZnO is a polar hexagonal, highly anisotropic crystal that grows along the c axis, (0001) because of the lowest surface energy of the (0002) facet [13]. The zinc and oxygen atoms in the ZnO crystal are arranged alternately along the c-axis, and the top surfaces are Zn terminated (0001) and are catalytically active, while the bottom surfaces are O-terminated ($000\bar{1}$) and are chemically inert [14]. Under hydrothermal conditions the polar (0001) faces are the most rapid-growth rate planes as compared to other growth

facets [13, 14] and hence the nanopencils morphology is preferred. Figure 1(c) shows the SEM image of PDMA nanostructures with well defined hexagonal morphology which is $\sim 3 \mu\text{m}$ in length and $\sim 160 \text{ nm}$ in diameter. The growth mechanism of these hexagonal structures is discussed in detail by Mavundla *et al.* [8]. PDMA-PPy in Figure 1 (d) shows spherical morphology with agglomerated particles.

3.2. X-ray Diffraction

The XRD patterns of PDMA, PDMA-PPy and ZnO are shown in Figure 2. Very sharp and strong peaks are observed at $2\theta = 11.8, 20.5, 26.5$ and 27° for PDMA, Figure 2(a). These strong peaks are an indication of a highly crystalline polymer material. The peaks at $2\theta = 26.5^\circ, 27^\circ$ and 20.5° can be ascribed to the periodicity parallel and perpendicular to the polymer chains of PANI, respectively [11]. The peak at 11.8° is an indication of a significant crystallization upon protonation [15]. The copolymer in Figure 2(b) shows a broad peak around $2\theta = 18-30^\circ$ which is due to an amorphous behaviour. The X-Ray patterns of ZnO are shown in Figure 2(c). The XRD pattern (Fig.2c) was indexed and compared with the JCPDS database (card No. 36-1451, $a = 3.249 \text{ \AA}$, $c = 5.206 \text{ \AA}$) [16]. It was determined that the product was a hexagonal wurtzite structure ZnO, showing a high crystallinity. The estimated value of the ZnO nanocrystallite size from the Scherrer formula [17] is 27.36 nm for pure powder.

3.3. Photoluminescence

The PL spectra of PDMA, PDMA-PPy, ZnO nanostructures and blended films are shown in Figure 3. There is a strong UV emission band around 390 nm for ZnO. This band is due to the band edge emission or radiative annihilation of excitons [18]. A blue band is observed around 430 and 460 nm , while a much stronger blue-green band located around 480 nm and a green band at 529 nm are observed. The blue-green band emission corresponds to a single occupied oxygen vacancy in ZnO. This results from the recombination of the photo-generated hole with a single ionized charged state of this defect [17, 19]. PL spectrum of the copolymer, PDMA-PPy shows bands at $390, 440$ and 480 nm , respectively. The peaks at 390 and 440 nm are due to the benzoic groups causing the emission in the different polymers. The small shoulder around 480 nm is due to the protonation form or the

dope state of the polymer [11, 20]. Poly(2,5-dimethoxyaniline) show a weak peak at 390 and a strong peak around 520 nm, which indicates that this material is more protonated and doped. This material is expected to perform better in the solar cells because of its broader absorption spectrum, which can result in better light harvesting. Upon blending the PDMA with ZnO in a 1:1 wt.%, the PL is quenched by a factor of 3 (reduction in the intensity of the spectrum), indicating a partial charge transfer between the ZnO and the PDMA. The PL spectrum of the blend also shows a blue shift (shift to higher energies or lower wavelengths). This blue-shift and the reduction in the PL intensity is probably due to an altering of the polymer structure.

3.4. Solar Cell Characterization

The current-voltage (I-V) characteristics of ITO/PDMA:ZnO/Al, ITO/PDMA:C₆₀/Al, and ITO/PDMA-PPy:C₆₀/Al is shown in Figure 4(a). The donor-acceptor ratio was kept at 1:1(w/w), and devices were measured at 800 mW under simulated AM 1.5 illumination. The photovoltaics parameters (V_{oc} , I_{sc} , FF, and PCE) of these devices are listed in Table 1. Comparing the performance of PDMA as a donor material when used with either ZnO or C₆₀ as an acceptor, it is evident from Fig.4 and Table 1 that the ZnO prepared devices exhibit a high PV performance with a open circuit voltage (V_{oc}) of 0.58 V, short circuit current density (I_{sc}) of 0.93 $\mu\text{A}/\text{cm}^2$, fill factor (FF) of 24.1 and an efficiency of 0.162%. A low efficiency is obtained for the PDMA:C₆₀ device, however it has a higher short circuit current density and fill factor compared to the PDMA:ZnO device. It is known that C₆₀ is a stronger electron acceptor material than ZnO, and is more efficient in charge separation which may lead to an enhancement of the photocurrent [21, 22]. It has been shown that the increase in photon harvesting from the solar spectrum results in a higher photocurrent [4, 7]. A higher open circuit voltage is obtained in the PDMA:ZnO devices. The origin of the V_{oc} in organic solar cells is not fully understood, it is widely believed to have a maximum value given by the difference in energy between the donor HOMO and acceptor LUMO [4], and in this study was not the case. The higher V_{oc} for the PDMA:ZnO was attributed to the fact that both ZnO and PDMA had one-dimensional morphology which enhances the charge separation and charge transport.

It is believed that the higher crystallinity as depicted in the XRD results may also be responsible for the high V_{oc} . When PDMA-PPy copolymer is used as a donor with ZnO as an

acceptor, a low power conversion efficiency of about $2.14 \times 10^{-4}\%$ was observed. The efficiency was improved by a factor of about 2 when using C_{60} as the electron acceptor material. This improvement can be attributed to the fact that spherical C_{60} molecules with larger surface to volume ratio are more efficient in separating the photogenerated charge carriers than one-dimensional structures when distributed in a polymer matrix [21].

4. CONCLUSION

Flower-shaped ZnO structures are synthesized by microwave annealing using the aqueous mixture of zinc nitrate and KOH at a low temperature of 180 °C. Nano-pencils grow out of the base of the ZnO flower-shaped structures. The X-ray diffraction patterns showed that these structures are wurtzite hexagonal ZnO. PDMA with hexagonal structures showed high power conversion efficiency due to its high crystallinity and smooth one-dimensional morphology. Applying these nano-pencils in a hybrid solar devices shows that the combination of one-dimensional structures and high crystalline materials is crucial for the improvement of solar cell performances. PL spectroscopy showed that an incorporation of ZnO in PDMA lead to a reduction in PL intensity and a blue shift.

5. ACKNOWLEDGEMENTS

The authors are grateful for the financial support of the Department of Science and Technology, South Africa and the Council for Scientific and Industrial Research (CSIR), South Africa (Project No. HGERA7S).

6. REFERENCES

- [1]. Tang, CW (1986) Appl Phys Lett 48: 183-185.
- [2]. Kim S-S, Jo J, Chun C, Hong J-C, Kim D-Y (2007) J Photochem Photobiol, A 188:364-370.
- [3]. Das NC, Sokol PE (2010) Renewable Energy 35:2683-2688.
- [4]. Dissanayake DMNM, Hatton RA, Lutz T, Giusca EC, Curry RJ, Silva SRP (2007) Appl Phys Lett 91:133506-133508.
- [5]. Briseno AL, Holcombe TW, Boukai AI, Garnett EC, Shelton SW, Frechet JJM, Yang P (2009) Nano Lett 10:334-340.
- [6]. Huynh WU, Dittmer JJ, Libby WC, Whiting GL, Alivisatos AP (2003) Adv Funct Mater 13:73-79.
- [7]. Kumar H, Kumar P, Bhardwaj R, Sharma GD, Chand S, Jain SC, Kumar V (2009) J Phys D: Appl Phys 42: 015103. doi:10.1088/0022-3727/42/1/015103.
- [8]. Mavundla SE, Malgas GF, Baker P, Iwuoha EI (2008) Electroanal 20:2347-2353.
- [9]. Chang M-Y, Wu C-S, Chen Y-F; Hsieh B-Z, Huang W-Y, Ho K-S, Hsieh T-H, Han Y-K (2008) Org Electron 9:1136-1139.
- [10]. Bejbouji H, Vignau L, Miane JL, Dang M-T, Oualim EM, Harmouchi M, Mouhsen A (2010) Sol Energy Mater Sol Cells 94:176-181.
- [11]. Mavundla SE, Malgas GF, Motaung DE, Iwuoha EI (2010) J Mat Sci 45:325-3330.
- [12]. Ahmad M, Zhu J (2011) J Mat Chem 21:599-614.
- [13]. Pol VG, Calderon-Moreno JM, Thiyagarajan P (2008) Langmuir 24:13640-13645.
- [14]. Ahsanulhaq Q, Kim SH, Kim JH, Hahn YB (2008) Mater Res Bull 43:3483-3489.
- [15]. Amarnath CA, Palaniappan S (2005) Polym Adv Technol 16:420-424.
- [16]. Xu F, Lu Y, Xie Y, Liu Y (2008) J Phys Chem C 113:1052-1059.
- [17]. Cullity D (1956) Elements of X-ray diffraction. Addison-Wesley, Massachusetts.
- [18]. Zheng ZX, Xi YY, Dong P, Huang GH, Zhou ZJ, Wu LL, Lin HZ (2002) Phys Chem Comm 5:63-65.
- [19]. Phuruangrat A, Thongtem T, Thongtem S (2009) Mater Lett 63:1224-1226.
- [20]. Shimano JY, MacDiarmid AG (2001). Synth Met 123:251-262.
- [21]. Sun JJ, Zhu Y, Yang X, Li C (2009) Particuology 7:347-352.
- [22]. Yildiz HB, Tel-Vered R, Willner I (2008) Adv Funct Mater 18:3497-3505.

List of Figures Captions and Tables

Figure 1: Scanning Electron microscopy images of (a) ZnO, (b) ZnO (higher magnification), (c) PDMA and (d) PDMA-PPy.

Figure 2: X-Ray Diffraction patterns of (a) PDMA, (b) PDMA-PPy and (c) ZnO.

Figure 3: Photoluminescence spectra of PDMA, PDMA-PPy, ZnO and PDMA blended with ZnO.

Figure 4: Current-voltage (I-V) characteristics of PDMA:ZnO, PDMA:C₆₀ and PDMA-PPy:C₆₀ devices.

Table 1: Photovoltaic device performances of different structures illuminated with a white light source.

Figure 1

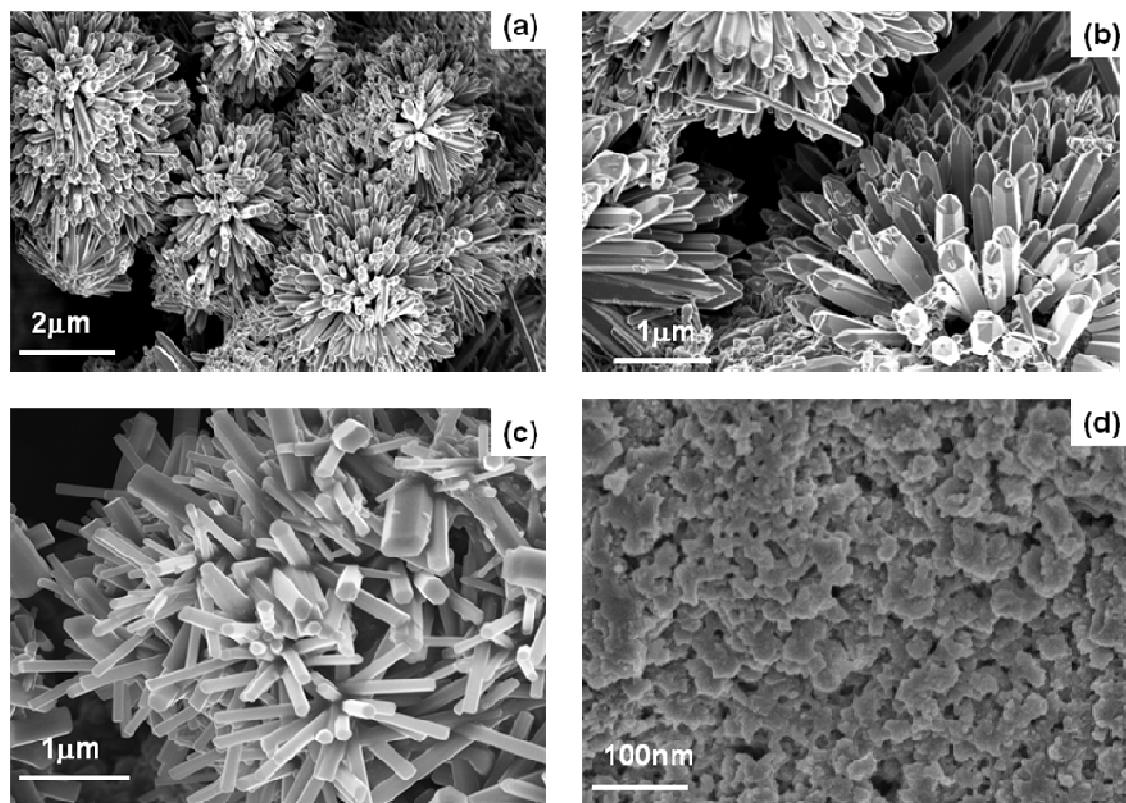


Figure 2

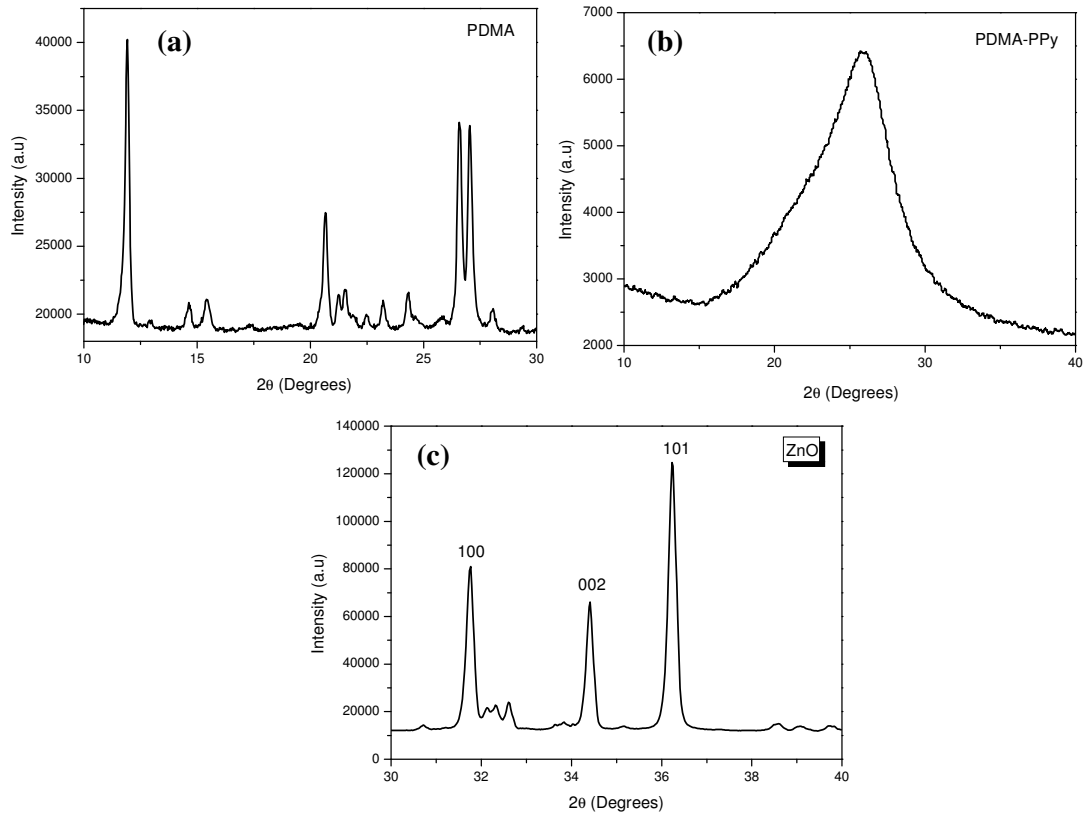


Figure 3

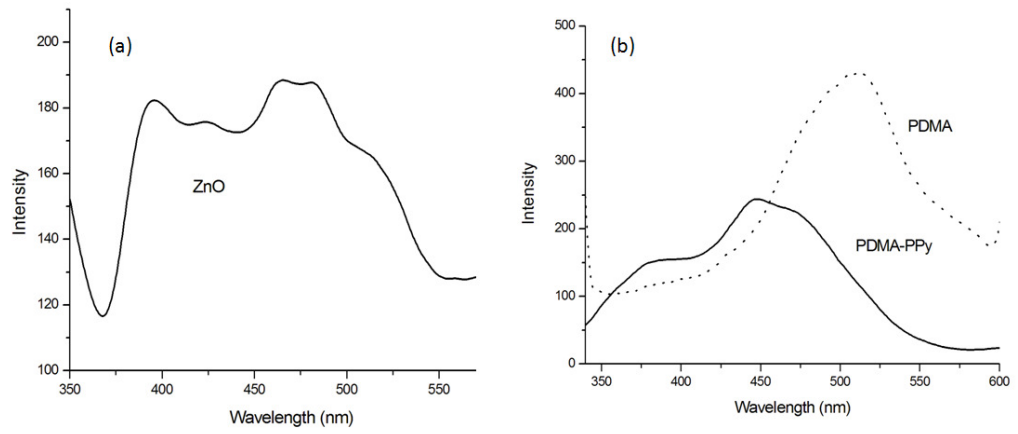


Figure 4

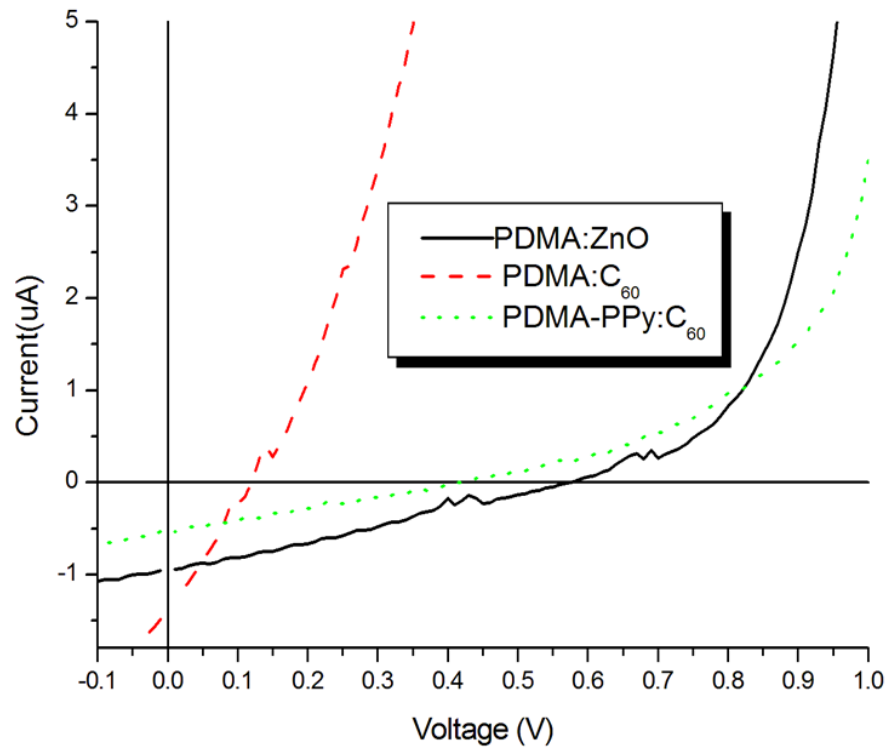


Table 1

Active layer	I_{sc} (μA)	V_{oc} (V)	FF %	CPE %
PDMA:ZnO	0.93	0.58	24.1	0.162
PDMA:C₆₀	1.39	0.12	24.5	0.051
PD-PPy:C₆₀	0.53	0.42	20	0.055
PD-PPy:ZnO	0.822	8.58 x10 ⁻⁴	24.3	2.14x10 ⁻⁴